RGNZ/MGPB

Thermal degradation of diverse rock suites: Insights from fractures and physical and mechanical analysis

Rudarsko-geološko-naftni zbornik
(The Mining-Geology-Petroleum Engineering Bulletin)
DOI: 10.17794/rgn.2025.4.4

Original scientific paper

Abid Nawaz[1]*, Muhammad Sajid[2,3], Waqas Ahmed[1], Abdul Rahim Asif[1,4]

[1] *National Centre of Excellence in Geology, University of Peshawar, Peshawar 25120, Pakistan.*
[2] *Department of Geology, University of Peshawar, Peshawar, 25120, Pakistan.*
[3] *Helmholtz-Zentrum Potsdam, Deutsches GeoForschungsZentrum (GFZ), Telegrafenberg, Potsdam, Germany.*
[4] *Department. of Geology, Fata University, FR Kohat 26100, Pakistan.*

Abstract

Understanding the effects of thermal treatment on the physical and mechanical properties of rocks is essential for evaluating their behaviour under extreme conditions and optimizing engineering designs. Thermal treatment significantly influences these properties, either enhancing or degrading them, depending on the mineralogical composition of the rocks. This study provides a detailed investigation into the thermal impact on the physical and mechanical properties of various rock types, including limestone, sandstone, granitic gneiss, rhyolite, quartzite, dolerite, gabbronorite, amphibolite, and granulite. The rock samples were exposed to heat treatment at temperatures ranging from 150°C to 1000°C. Subsequently, destructive (uniaxial compressive strength, point load index) and non-destructive tests (specific gravity, ultrasonic pulse wave velocity, porosity, and water absorption) were conducted to assess the rocks' responses to varying temperatures. The density of thermally induced fractures is calculated for each rock type at the investigated temperatures. The results indicate a reduction in uniaxial compressive strength, specific gravity, ultrasonic pulse velocity, and point load strength as the temperature increases. Conversely, elevated temperatures increased fracture density, porosity, and water absorption levels. A noticeable and abrupt change in all properties is observed when the temperature exceeds 300°C. These results highlight the deterioration of rocks and the alterations in their physical and mechanical properties caused by heat exposure, which hold critical importance for industries like mining and construction. Combining the physical and mechanical test results at different temperature levels, equations were derived for each rock type that can be used to estimate the respective properties at the desired temperatures. This study is significant for understanding how thermal exposure affects the integrity of rocks, providing crucial understanding for industries such as mining, construction, and geothermal energy. It enables better prediction and management of rock behaviour under high-temperature conditions, enhancing safety and performance in engineering applications.

Keywords:
heat treatment, thermal impact, physical and mechanical properties, rock suites, thermal degradation, equations

1. Introduction

Rock is often perceived as an "eternal" material (**Brotóns et al., 2013**). The intrinsic properties of the natural rocks should be thoroughly investigated, especially before considering them for civil structures such as highways, bridges, and tunnels (**Sajid et al., 2016; Asif et al., 2022, 2024**). Rocks have undergone various processes of deterioration during their geological evolution; hence it is important to understand their behaviour against different aggressive agents (**Asif et al., 2021**). Temperature is one such important factor that affects the physical and mechanical properties of natural rocks (**Si et al., 2024; Huang et al., 2025**).

The mechanical behaviour of rocks under high-temperature conditions is critically important for applications such as deep geological disposal of nuclear waste (**Wang et al., 2024; Kibikas et al., 2025**), hot dry rock (HDR) geothermal energy extraction (**Yin et al., 2024; Jiang et al., 2025**), and underground coal gasification (**Li et al., 2024; Shahbazi et al., 2024**). Understanding these variations provides essential insights into deformation, stability, and safety analyses for such projects. Elevated temperatures can cause thermal expansion of rock-forming minerals, induce thermal stresses, and trigger chemical reactions within the rock, resulting in micro-crack formation and damage to microstructures (**Zhang et al., 2024**). Generally, rock strength and deformation modulus tend to decline as temperature increas-

* Corresponding author: Abid Nawaz
e-mail address: abidgeo88@uop.edu.pk
Received: 6 December 2024. Accepted: 21 February 2025.
Available online: 27 August 2025

es, particularly beyond a critical threshold (**Feng et al., 2023; Wong et al., 2024**).

High-temperature exposure modifies the microstructural characteristics of rocks by generating new microcracks, which increase the overall void volume (**Hu et al., 2024; Wu et al., 2025**). The extent of these thermally induced microcracks (inter- or intra-granular) is influenced by the properties of the constituent minerals (**Pan et al., 2024**). Studies by **Gomah et al. (2024)** and **Long et al. (2024)** have examined micro-fractures and thermal damage in granite subjected to temperatures up to 600°C. Heat-induced strength reduction is primarily attributed to the propagation of existing microcracks and the development of new cracks caused by temperature variations (**Ma et al., 2024**). Additionally, models such as those proposed by **Qiao et al. (2024)** utilize the modulus of elasticity to calculate damage parameters for rocks under heat treatment.

The geological settings of northern Pakistan (see **Figure 1**) offer a diverse array of rock units. This study investigates nine texturally and geochemically diverse rock types from different tectonic domains for thermally induced cracking. Previous relevant studies have primarily focused on granites or limestones due to their excessive use in construction projects (**Khan and Sajid, 2023**). In addition to granitic gneiss from the Hazara region and limestone from the Nowshera Formation in northern Pakistan, this study explores other rock types for the first time to gain better control over the textural and mineralogical responses to thermal cracking during heat treatment. These include gabbronorite, granulite, and amphibolite from the southern units of Kohistan Island Arc (KIA), volcanics from the Upper Dir regions (Northern KIA), dolerite from the Gadoon Amazai, quartzite from the Tanawal Formation in the Indian plate sequence, and sandstone from the Murree Formation (see **Figure 1**).

The scientific contribution of this research lies in expanding the scope of thermal studies by analyzing less-studied rock types such as gabbronorite, granulite, amphibolite, dolerite, volcanics, quartzite, and sandstone. It establishes new correlations between temperature-induced microcrack evolution and the mineralogical and textural properties of diverse rock types. Additionally, the study develops predictive mathematical models for rock damage under thermal treatment, offering a quantitative approach for assessing rock stability in high-temperature engineering applications, such as geothermal energy extraction, nuclear waste disposal, and underground coal gasification. Furthermore, this research provides a comparative analysis of rock behaviour across different tectonic settings, particularly from the Eurasian Plate, the Kohistan Island Arc, and the Indian Plate, contributing to a better understanding of regional geological materials under thermal stress. By integrating petrographic, mechanical, and statistical analyses, this study advances knowledge on the thermal durability and degradation mechanisms of various rock types, offering practical insights for geotechnical and engineering applications.

2. Geology of northern Pakistan

Northwestern Pakistan consists of three primary tectonic domains: the Indian Plate, the Kohistan Island Arc (KIA), and the Eurasian Plate. The KIA formed through intra-oceanic subduction within the Tethys Ocean and subsequently collided with the Indian Plate along the Main Mantle Thrust (MMT) (see **Figure 1**) (**Searle and Treloar, 2010; Burg, 2018**). To the north, the KIA is bounded by the Main Karakoram Thrust (MKT). Its composition reflects two major collision events: one with the Eurasian Plate and another with the Indian Plate, leading to intricate deformation and metamorphism (**Zeitler, 1985; Treloar et al., 1989; Searle et al., 1999**). The KIA is divided into six main units from south to north, consisting of sedimentary, volcanic, and plutonic rocks (**Khan et al., 1993; Arif and Jan, 2006; Sajid et al., 2018**).

The deepest part of the Kohistan Paleo-Island Arc comprises the mafic and ultramafic Jijal Complex, which represents the transitional zone between the upper mantle and lower crust (**Jan and Howie, 1981; Bard, 1983; Ringuette et al., 1999; Dhuime et al., 2007**). The gabbroic and mafic-to-intermediate metavolcanics in this region underwent metamorphism to amphibolite facies, forming the Kamila Amphibolite Belt (**Coward et al., 1987**). To the north of the Kamila Amphibolite lies the Chilas Complex, a large magmatic body from the Late Cretaceous primarily composed of gabbronorite, with minor occurrences of troctolite, quartz diorite, and gabbro (**Treloar et al., 1996**).

The Kohistan Batholith contains Early Cretaceous Chalt Volcanics, including andesitic lavas, tuffs, and agglomerates, as well as calc-alkaline granitoids (**Ringuette et al., 1999; Dhuime et al., 2007**). In the northern KIA, the Yasin and Chalt group rocks consist of volcaniclastic rocks, greywackes, and pelites (**Jan and Howie, 1981; Jan, 1988**). To the south, the northern Indian Plate is divided into three tectonic units: the Lesser Himalayan Sequence (LHS), the Greater Himalayan Sequence (GHS), and the Tethyan Himalayan Sequence (THS). These units are separated by two major fault systems: the Main Central Thrust (MCT) and the South Tibetan Detachment System (STDS) (see **Figure 1**).

Additionally, various granitic suites have been identified within the Himalayan terrane. These include early Cenozoic granitoids associated with the Himalayan collision (**King et al., 2011; Searle, 2011**), late Paleozoic granitoids linked to rift-related processes (**Noble et al., 2001**), and early Paleozoic granitoids formed during accretionary orogenesis (**Le Fort, 1986; Cawood et al., 2007; Wang et al., 2013**).

3. Experimental campaign

3.1. Sample preparation and heat treatment

The sample locations, mineralogy, and a brief petrographic description of the studied rocks are summarized

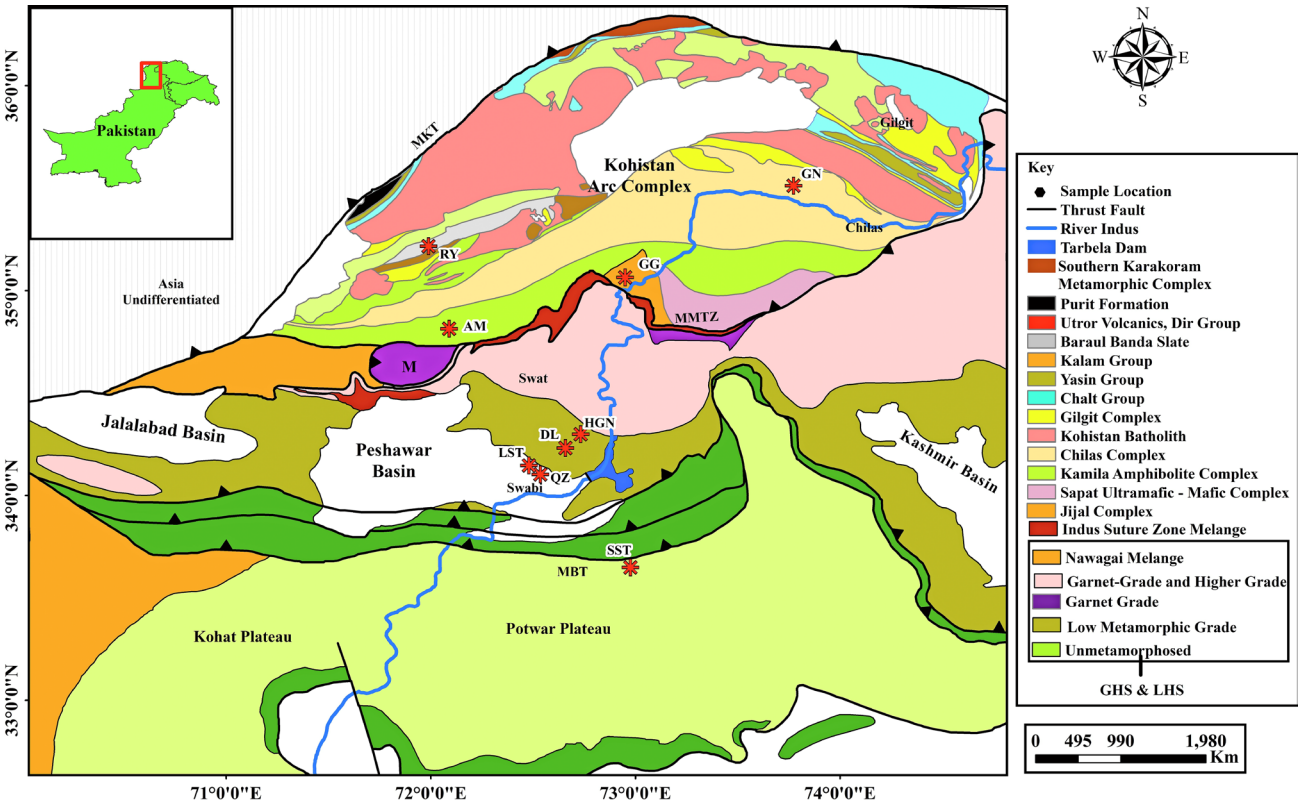

Figure 1. Geological Map of the Western Himalayas in Pakistan, adapted from **DiPietro et al. (2008)**. The red stars indicate the locations of the studied samples, with corresponding geological formations labelled: RY (Rhyolite from Utror Volcanics), AM (Amphibolite from Kamila Amphibolite), DL (Dolerite from Panjal Dykes), LST (Limestone from Nowshera Formation), QZ (Quartzite from the Tanawal Formation), HGN (Hazara Granitic Gneiss), SST (Sandstone from Murree Formation), GN (Gabbronorite from Chilas Complex), GG (Granulite from Jijal Complex).

in **Table 1**. Bulk rock samples were collected during fieldwork from various areas in northern Pakistan (see **Figure 1**). These samples were cut into cubes measuring 5.08x5.08x5.08 cm at the National Centre of Excellence in Geology (NCEG), University of Peshawar. The cubic specimens were subjected to a range of temperature treatments, starting from room temperature and progressing to higher levels: 150°C, 300°C, 600°C, 800°C, and 1000°C. This was done to evaluate the physical and mechanical changes induced by temperature variations.

The specimens were heated in a furnace with a controlled rate of 2°C per minute until the target temperature was reached. Each sample was maintained at the specified temperature for 24 hours before being gradually cooled to room temperature. Additionally, one sample from each rock type was preserved at room temperature as a control for comparative analyses.

3.2. Physical and mechanical testing

Following the thermal treatment, the rock cubes exposed to each temperature were subjected to both destructive and non-destructive tests to assess changes in their physical and mechanical properties. The testing procedures adhered to the American Society for Testing and Materials (ASTM) standards for physical (specific gravity, water absorption, porosity, and ultrasonic pulse velocity) and mechanical (unconfined compressive strength and point load test) evaluations.

Ultrasonic pulse velocity (UPV) was measured using a pitch-catch technique with a pair of transducers (transmitter and receiver) in accordance with ASTM-D-2845-08. The samples were weighed in various states: air-dried, oven-dried, submerged in water, and water-saturated after 24 hours. Bulk water absorption, bulk saturated specific gravity (DC97/C97M-18), and bulk porosity were then calculated using the following formulas:

$$\text{Water absorption} = \frac{(\text{Water saturated weight} - \text{Dry weight})}{\text{Dry weight}} \quad (1)$$

$$\text{Specific gravity} = \frac{\text{Saturated weight}}{(\text{Saturated weight} - \text{Weight in water})} \quad (2)$$

$$\text{Porosity} = \frac{(\text{Weight in air} - \text{Dry weight})}{(\text{Weight in air} - \text{Weight in water})} \quad (3)$$

The unconfined compressive strength (UCS) (ASTM D7012–14e1) and point load testing (PLT) (ASTM D 5731) were also conducted on the samples at each investigated temperature level. Formula for the both is given below:

Table 1. Symbols, Geological Locations, Mineralogical Composition, and Textural Descriptions of Investigated Rocks

S. No	Rock	Symbol	Geological Unit	Coordinates	Mineralogy	Grain Size
1	Dolerite	DL	Panjal Dykes	34.23113000, 72.65824833	Plagioclase, Augite, Olivine, Hornblende	Medium grained
2	Rhyolite	RY	Dir Volcanics (KIA)	35.21587866, 71.98874537	Quartz, K–feldspar, Biotite	Fine grained
3	Gabbronorite	GN	Chilas Complex	35.511531, 73.773089	Plagioclase, Orthopyroxene, Clinopyroxene	Coarse grained
4	Sand stone	SST	Murree Formation	33.64813945, 72.97608807	Quartz, Feldspar, Matrix	Coarse grained
5	Limestone	LST	Nowshera Formation	34.14549205, 72.47979880	Calcite	Fine grained
6	Quartzite	QZ	Tanawal Formation	34.10182333, 72.53580833	Quartz, Feldspar	Medium to Coarse grained
7	Granitic gneiss	HGN	Hazara Granitic Gneiss	34.29825500, 72.73238000	Quartz, Orthoclase, Plagioclase, Biotite, Muscovite	Coarse grained and strongly foliated
8	Amphibolite	AM	Kamila Amphibolite	34.94245500, 72.02215000	Hornblende, Plagioclase Quartz, Epidote	Coarse grained
9	Granulite	GG	Jijal Complex	35.063864, 72.949761	Pyroxene, Biotite, Garnet, Plagioclase	Medium to Coarse grained

$$UCS = \frac{P}{A} \tag{4}$$

Where P is the failure load, and A is the cross-sectional area of the core sample.

3.3. *Fracture demarcation*

Thin sections were prepared from the samples at room temperature and each treatment temperature, enabling a closer examination of their internal structure and respective variations. Photomicrographs were captured from the thin sections, providing visual records for analysis. The ImageJ software is employed to outline the individual fractures observed in the photomicrographs of treated samples subjected to different temperatures, which are then compared with photomicrographs of untreated samples (room temperature). The area and extent of each fracture present in the photomicrographs were precisely calculated. Additionally, the total area of the rock specimen mounted on a thin section was derived. The fracture density is calculated using the following formula:

$$\text{Fracture density} = \\ = 100\% - (\text{Area of thin section-Area of Fractures}) / \\ / \text{Area of thin section}*100 \tag{5}$$

Certain features were considered while examining thin sections to identify thermal cracks. Firstly, the presence of distinct fracture patterns between the treated and untreated samples is noted, such as irregular or straight lines that intersect or traverse the rock matrix. These cracks may appear as dark isotropic lines or discontinuities in the thin section. Another important clue is the presence of iron leaching near the fractures, resulting in noticeable colour changes or staining patterns during treatment. Thermally-induced cracks display extensive discontinuities that cut across multiple mineral grains in the thin section, which is not the case in untreated samples. These fractures exhibit irregular and jagged patterns, setting them apart from other types of discontinuities or cleavages. **Figure 2** represents the photomicro-

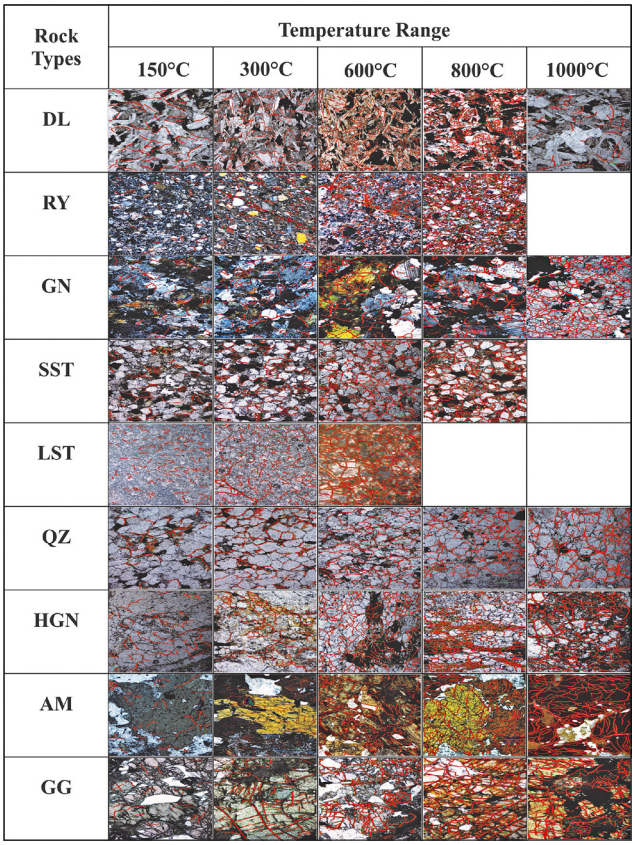

Figure 2. Fracture Demarcation of the Studied Samples After Thermal Treatment

graphs of the all studied samples treated at different temperatures, in which fractures are marked with red lines.

4. Results

4.1. Thermally induced fractures

The increase in fracture density in the investigated samples with increasing temperature is noted, as shown in **Figure 3**.

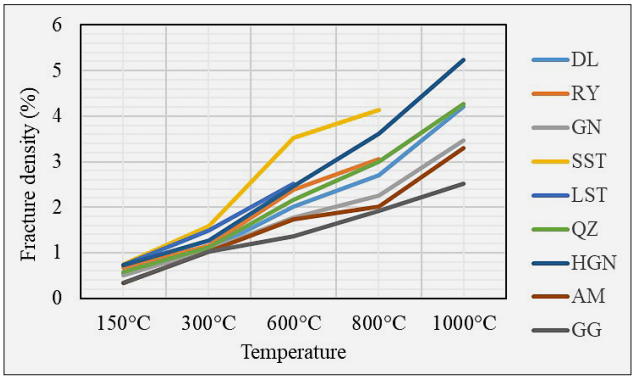

Figure 3. Fracture Density Variation in Investigated Rock Samples Across Different Temperatures

At 150°C, the fracture density of dolerite is 0.54%, rhyolite is 0.67%, gabbronorite is 0.5, sandstone is 0.75, limestone is 0.73, quartzite is 0.58, granitic gneiss is 0.72, amphibolite is 0.34%, and granulite is 0.33%. As temperature rises, fractures become more extensive, and their intensity increases. The fracture density of the aforementioned samples reached 2.01%, 2.38%, 1.77%, 3.52%, 2.51%, 2.17%, 2.46%, 1.74%, and 1.36%, respectively, at 1000°C (see **Figure 4**). Granulite proves to be the most resistant to thermal deterioration, while limestone and sandstone deteriorate at 600°C and 800°C respectively. Moreover, the rhyolite sample becomes very fragile at 1000°C, and a thin section cannot be extracted from it as it erodes completely during the process; hence, the fracture density for rhyolite is not calculated at this temperature.

The increase in fracture density of rock samples after their exposure to higher temperatures is shown in **Figure 4**

4.2. Unconfined Compressive strength (UCS)

Figure 5A shows the UCS values recorded at various temperatures (25°C to 1000°C). Limestone exhibits a relatively gentle decline in strength during testing; however, it completely disintegrates at 600°C. Sandstone has lower strength than limestone at all temperatures; however, interestingly, it survives more than limestone during treatment till 800°C, after which it completely fragments. Granulite demonstrates the highest resilience among all the studied samples and exhibits the highest

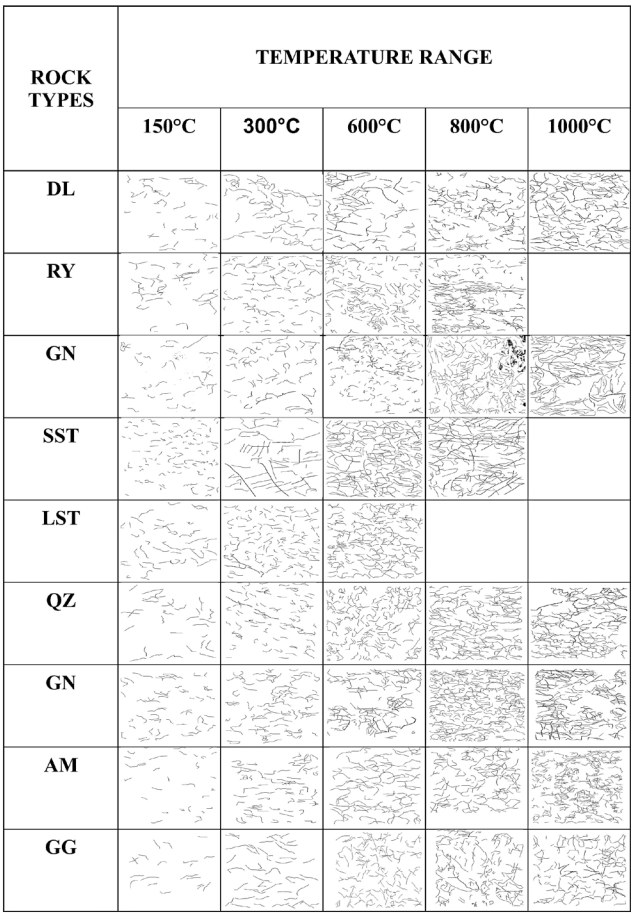

Figure 4. Fracture Distribution in studied rocks across different temperatures

strength at all temperatures (see **Figure 5A**). Additionally, the overall percentage decrease in its strength from room temperature to 1000°C is lower than that of other rock types. The UCS of dolerite reduced to 82% at 1000°C relative to room temperature, rhyolite to 87%, gabbronorite to 80%, quartzite to 84%, granitic gneiss to 89%, amphibolite to 77%, granulite to 74%. As mentioned earlier, the limestone and sandstone deteriorated before 1000°C. The UCS of limestone reduced to 71% at 600°C, and there was a total reduction of 89% in the UCS of sandstone at 800°C.

4.3. Point load (PLT)

The experimental findings indicate a noticeable effect of temperature on the point load strength of the rock samples tested. At first, a slight change in point load strength is observed as the temperature increases from room temperature to 150°C (see **Figure 5B**). However, as the temperature range exceeds, a notable and significant decrease in point load strength is noted (see **Figure 5B**). At the highest investigated temperature (1000°C), there is a reduction of 75% in the point load strength of dolerite, 86% in rhyolite, 72% in gabbronorite, 81% in quartzite, 89% in granitic gneiss, 67% in amphibolite and 63% in granulite. Moreover, limestone experienced

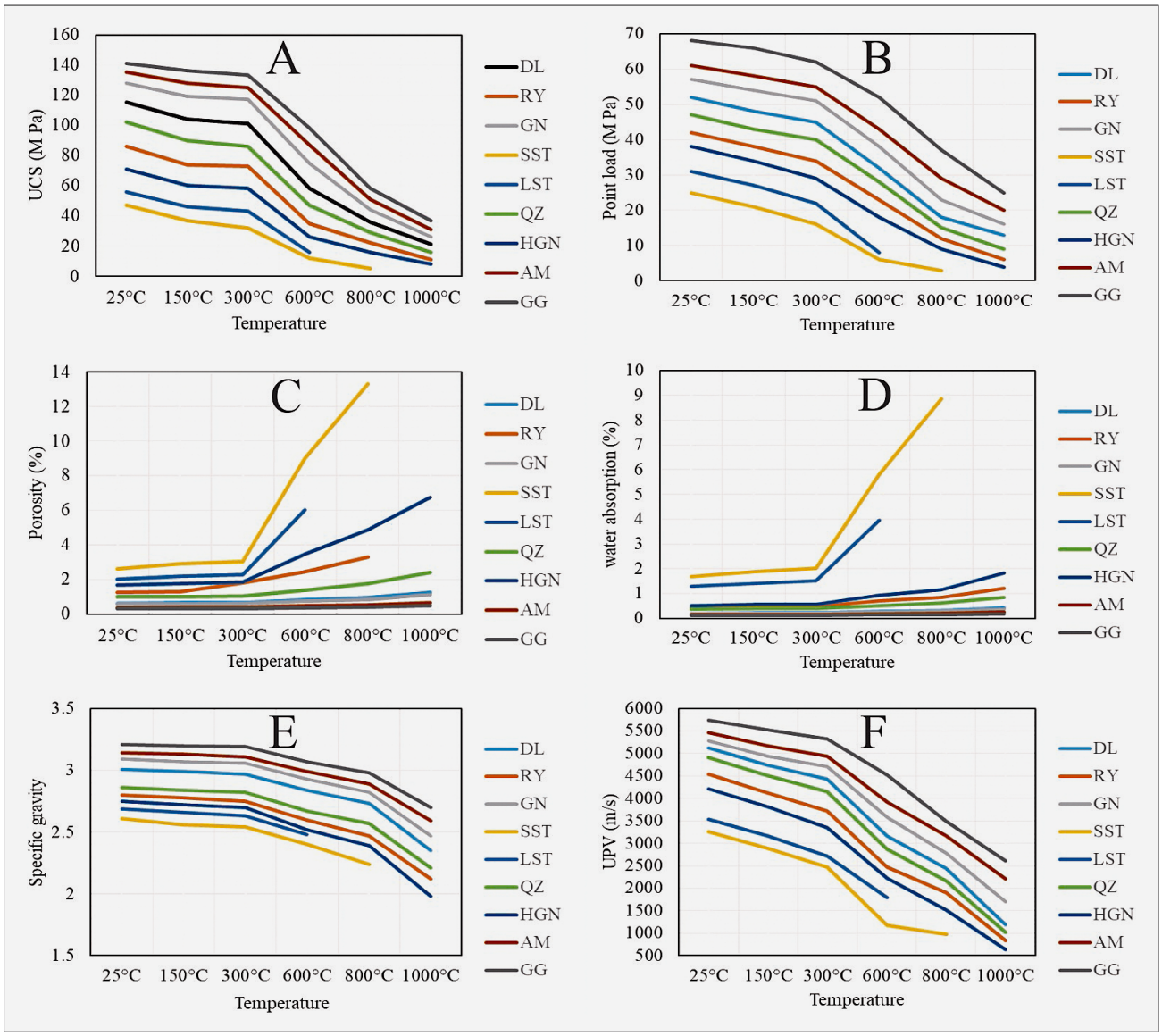

Figure 5. Influence of Temperature on Physical and Mechanical Properties of Rocks: **(A)** Uniaxial Compressive Strength (UCS); **(B)** Point Load; **(C)** Porosity; **(D)** Water Absorption; **(E)** Specific Gravity; **(F)** Ultrasonic Pulse Velocity (UPV).

74% reduction at 600°C and sandstone experienced 88% at 800°C.

4.4. Porosity, Water absorption, and Specific gravity

Figure 5C represents the result of porosity tests at the investigated temperatures in this study. The porosity of the samples exhibited an overall increase with increasing temperature, evidently because of an increase in fracture intensity. The porosity values of dolerite, rhyolite, gabbronorite, quartzite, granitic gneiss, amphibolite, and granulite increased up to 52%, 64%. 49%, 59%, 75, 41%, and 38% respectively at 1000°C. Moreover, there is an increase of 67% in the porosity of limestone at 600°C and 80% in sandstone at 800°C. Similar increases are also noted with water absorption values (see **Figure 5D**). The percentage increase in water absorption of dolerite, rhyolite, gabbronorite, quartzite, granitic gneiss, amphibolite, and granulite is 51%, 65%, 49%, 58%, 72%, 42%, and 35% respectively, at 1000°C. Furthermore, the water absorption of limestone increases to 67% at 600°C, and sandstone increases to 81% at 800°C.

The test results demonstrate that specific gravity is influenced by temperature variations, as represented in **Figure 5E**. A noticeable decrease is shown with increasing temperature. The percent decrease in the studied samples of dolerite, rhyolite, gabbronorite, quartzite, granitic gneiss, amphibolite, and granulite is 30%, 24%, 20%, 23%, 28%, 18%, and 16% respectively, at 1000°C. The specific gravity of limestone decreased up to 8% at 600°C and sandstone upto14% at 800°C.

4.5. Ultrasonic pulse velocity (UPV)

Experimental findings demonstrate a consistent decrease in UPV values with increasing temperature (see

Figure 5F). A slight variation in UPV was observed initially; however, a significant decrease in UPV occurred when the temperature exceeded 600°C. For instance, the percent UPV values of dolerite, rhyolite, gabbronorite, quartzite, granitic gneiss, amphibolite, and granulite reduced up to 77%, 82%, 68%, 79%, 85%, 56% and 55% respectively, at 1000°C. There is also a reduction of 49% in UPV of limestone at 600°C and 70% in sandstone at 800°C. These findings highlight the temperature-dependent effects on water absorption, porosity, specific gravity and UPV. Moreover, it emphasizes the importance of considering temperature variations when assessing the mechanical properties and integrity of rocks.

The detailed quantitative results of the studied rocks, including UCS, PLT, UPV, fracture densities, porosity, water absorption, specific gravity, and calculated Thermal Damage (DT) values are comprehensively presented in **Tables 1–5 in the supplementary file**.

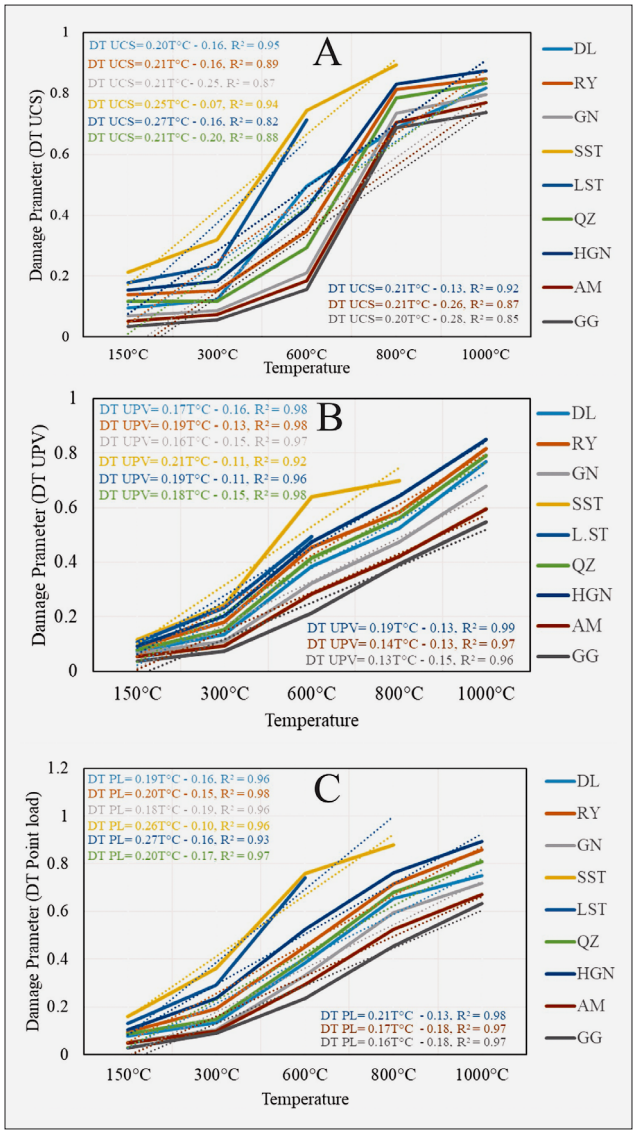

Figure 6. Thermal Damage Parameters in Different Rock Samples Across Varied Temperature Ranges: **(A)** Uniaxial Compressive Strength (UCS); **(B)** Ultrasonic Pulse Velocity (UPV); **(C)** Point Load

5. Discussion

Ozguven and Ozcelik (2013) studied the impact of various temperature levels, from room temperature to 1000°C, on marble and limestone. Their research examined changes in colour, whiteness, polish quality, daily physical properties, and pH. The results showed that natural stone starts to degrade and develop cracks when exposed to temperatures above 800°C. While the effects of high temperatures on the mechanical properties of rocks are generally agreed upon, variations in mineral composition, textural relationships, the thermal behaviour of individual minerals, and the nature of fractures and deformation contribute to the differences in mechanical characteristics affected by temperature.

5.1. Thermally induced fracturing

Research has also shown that high temperatures can alter the mineralogical properties of rocks (**Kanu et al., 2008; Yavuz et al., 2010; Vázquez et al., 2015**). Numerous studies have focused on how temperature affects thermal cracking in rocks and the subsequent impact of these micro-cracks on the rock structure. For instance, newly formed micro-cracks have been found to signifi-

Table 2. Equations Derived for the Estimation of Uniaxial Compressive Strength (UCS), Ultrasonic Pulse Velocity (UPV), and Point Load Values of Rocks at Specific Temperature Conditions

ROCK SAMPLE	UCS(T)	PL(T)	UPV(T)
DL	$UCS_{(0)}$(1- 0.20 x T°C - 0.16)	$PL_{(0)}$(1-0.19 x T°C - 0.16)	$UPV_{(0)}$(1-0.17x T°C - 0.16)
RY	$UCS_{(0)}$(1-0.21xT°C - 0.16)	$PL_{(0)}$(1-0.20x T°C - 0.15)	$UPV_{(0)}$(1-0.19x T°C - 0.13)
GN	$UCS_{(0)}$(1-0.21x T°C - 0.25)	$PL_{(0)}$(1-0.18x T°C - 0.19)	$UPV_{(0)}$(1-0.16x T°C - 0.15)
SST	$UCS_{(0)}$(1-0.25x T°C - 0.07)	$PL_{(0)}$(1-0.26x T°C - 0.10)	$UPV_{(0)}$(1-0.21x T°C - 0.11)
LST	$UCS_{(0)}$(1-0.27x T°C - 0.16)	$PL_{(0)}$(1-0.27x T°C - 0.16)	$UPV_{(0)}$(1-0.19x T°C - 0.11)
QZ	$UCS_{(0)}$(1-0.21x T°C - 0.20)	$PL_{(0)}$(1-0.20x T°C - 0.17)	$UPV_{(0)}$(1-0.18x T°C - 0.15)
HGN	$UCS_{(0)}$(1-0.21x T°C - 0.13)	$PL_{(0)}$(1-0.21x T°C - 0.13)	$UPV_{(0)}$(1-0.19x T°C - 0.13)
AM	$UCS_{(0)}$(1-0.21x T°C - 0.26)	$PL_{(0)}$(1-0.17x T°C - 0.18)	$UPV_{(0)}$(1-0.14x T°C - 0.13)
GG	$UCS_{(0)}$(1-0.20x T°C - 0.28)	$PL_{(0)}$(1-0.16x T°C - 0.18)	$UPV_{(0)}$(1-0.13x T°C - 0.15)

cantly weaken rocks (**Ferrero and Marini, 2001; Chaki et al., 2008; Chen et al., 2012**). These investigations demonstrated that both increases and decreases in temperature can lead to damage marked by cracking, which in turn reduces the rocks' strength (**Huang and Xia, 2015; Ersoy et al., 2019**).

Recent studies have led to the development of empirical models aimed at estimating the thermal damage to rocks at varying temperatures (**Rong et al., 2018; Sirdesai et al., 2018**). In these studies, rocks were typically exposed to high temperatures up to 1000°C to determine the threshold of thermal damage. In the current investigation, when comparing different rock samples, it was observed that granulite exhibited less fracture propagation during heat treatment compared to other rock types. Conversely, granitic gneiss showed a pronounced increase in fracture propagation from 150°C to 1000°C, in comparison to other types of rock. This behaviour can be attributed to the foliated structure present in granitic gneiss at room temperature, which likely contributes to the rapid propagation of fractures. Fracture initiation occurred soon after the thermal treatment began and became more significant at higher temperatures (see **Figure 4**). As the temperature increased, thermal cracking initiated, with its density rising at elevated temperatures (see **Figure 3**).

5.2 Calculation of Thermal damage

The mechanical strength of rocks decreases considerably when they are exposed to higher temperatures due to the internal thermal damage via fracturing. Using the UCS, UPV and point load results of thermally tested rock samples, the thermal damage of each rock type has been calculated using following formula (**Ersoy et al., 2019**).

$$(DT)\ UCS = 1 - UCS(T) / UCS(0) \quad (6)$$

$$(DT)\ UPV = 1 - UPV(T) / UPV(0) \quad (7)$$

$$(DT)\ PL = 1 - PL(T) / PL(0) \quad (8)$$

where DT is thermal damage, UCS(T) is the UCS of the sample exposed to T°C, UCS (0) is the UCS of the samples at room temperature, UPV(T) is the UPV of the sample exposed to T°C, UPV (0) is the UPV of samples at room temperature, PL(T) is point load at specific temperature, while PL (0) is point load at room temperature.

Figure 6 presents the thermal damage corresponding to UCS, UPV and PL derived from the above equation for each rock type at the investigated temperature which has been subsequently plotted against respective temperature in **Figures 6A, 6B** and **6C** respectively. These corresponding linear equations for each rock have been combined with eq. 1, 2 and 3, and subsequently, new equations have been acquired for the prediction of UCS, UPV, and PL values at any designated temperature (see **Table 2**). We recommend the use of these equations for the estimation of mechanical parameters of rocks at certain temperatures.

5.3. Effects of temperature on physical and mechanical strength of rocks

This study examined the thermal effects on various rock types by observing changes in their physical and mechanical properties and conducting petrographic analyses after thermal treatment at temperatures ranging from room temperature to 1000°C. The development of new micro-cracks has been shown to substantially reduce rock strength (**Chen et al., 2012; Ferrero and Marini, 2001; Lion et al., 2005**). It has been observed that rocks can lose about 50% of their initial strength when exposed to temperatures above 500-600°C, with the extent of loss influenced by their texture and mineral composition (**Chaki et al., 2008; Zhang et al., 2009**). Similarly, the samples in this study exhibited thermally induced cracking and an increase in fracture density as the temperature rose (see **Figure 3**). An increase in temperature also significantly impacts the point load strength of studied rocks. The granulite displays evident resistance to thermal deterioration, while limestone and sandstone show indications of deterioration even at lower temperature thresholds, as shown in **Figure 5**.

All rock types show a slight decrease in the compressive strength from room temperature up to 300°C. However, the curve shows a steep declining drift from 300°C to 600°C and subsequently to 800°C (see **Figure 5A**). Further, up to 1000°C, it is not as sharp as noted from 300°C to 800°C. This UCS curve analysis evidently shows the unstable response of the mineralogical composition and textural relation of the minerals to the heat treatment between 300°C to 800°C. Another important observation is that this behaviour is uniformly noted in all the rock types, irrespective of the rock composition and textural relations. The study samples exhibit a broad range of compositional (igneous, metamorphic and sedimentary) and textural relations ranging from fine-grained (rhyolites and limestone) to coarse grained (gabbronorite, amphibolite) rocks and massive (dolerite) to foliated (granitic gneiss) rock types. This shows that heat treatment reduces the strength of rocks, irrespective of their composition and textural characteristics.

Comparing the individual rock types, the granulite exhibits greater strength than all at room temperature, while sandstone yielded the lowest (see **Figure 5A**). Although the investigated limestone proved to be stronger (56 MPa) than the studied sandstone (47 MPa) at room temperature, its strength collapses with heat at 600°C, while the sandstone shows more steadiness till 800°C.

The sedimentary rocks examined in the current study include sandstone and limestone, both of which yield the lowest strength at room temperature and subsequent higher temperatures. Sedimentary rocks are formed at relatively lower temperature conditions (< 300°C) in

comparison to igneous (gabbronorite, dolerite) and metamorphic (quartzite, gneiss, amphibolite, granulite) rocks. The failure of limestones and sandstones can be explained by their low-temperature petrogenetic process, where all the other rock types are exposed to higher temperatures during the process of their formation and thus respond in a relatively stable manner to higher temperature. The point load strength varies among the studied rocks mostly in a similar pattern as UCS (see **Figure 5B**).

The temperature has significant impacts on the porosity of rocks, with an overall increase observed as the temperature rises (see **Figure 5C**). Similarly, the water absorption of rock samples shows a direct positive correlation with temperature, increasing gradually as the temperature rises (see **Figure 5D**). The trend of porosity and water absorption versus temperature is minimal till 300°C, most probably due to the sintering effect. However, an abrupt significant increase is noted during treatment at > 300°C (see **Figures 5C** and **5D**). This shows a widening of thermal cracks beyond this temperature, which has also been supported by the fracture density calculated at each investigated temperature (see **Figure 4**). The specific gravity and UPV decreases as temperature rises (see **Figures 5E and 5F**). As noted in other investigated properties, sharp change in both SG and UPV is noted at 300°C. All these analyses demonstrate a significant alteration in the behaviour of minerals and textural relations beyond 300°C during the heat treatment process.

6. Conclusions

This research examined how temperature affects the physical and mechanical properties of rocks, such as water absorption, specific gravity, porosity, and UPV. Different samples of igneous, sedimentary, and metamorphic rocks were exposed to a broad temperature range from 25°C to 1000°C, and their properties were evaluated following heat treatment and subsequent cooling. The results revealed temperature-dependent variations in the mechanical behaviour of rocks which highlight the importance of considering temperature effects prior to recommendations for geological and engineering purposes. The major outcomes can be summarized as:

- During the heat treatment of rock types, a significant shift in the physical and mechanical properties is observed when the temperature exceeds 300°C properties. This temperature can be considered a critical threshold for rocks during thermal exposure.
- The critical temperature investigated is not dependent on any compositional and textural characteristics of rocks, as it is uniformly applicable in all cases.
- The equation derived from the physical and mechanical results of the investigation can be applied to estimate the respective property at any anticipated temperature. However, variations may occur due to changes in the alteration grade of rock.

Acknowledgement

The authors would like to acknowledge the National Centre of Excellence in Geology at the University of Peshawar (Pakistan) for providing laboratory facilities and field logistics.

7. References

Arif, M., Jan, M.Q. (2006). Petrotectonic significance of the chemistry of chromite in the ultramafic–mafic complexes of Pakistan. Journal of Asian Earth Sciences, 27(5), 628-46. https://doi.org/10.1016/j.jseaes.2005.06.004

Asif, A.R., Islam, I., Ahmed, W., Sajid, M., Qadir, A., Ditta, A. (2022). Exploring the potential of Eocene carbonates through petrographic, geochemical, and geotechnical analyses for their utilization as aggregates for engineering structures. Arabian Journal of Geosciences, 15, 1–19. https://doi.org/10.1007/s12517-022-10383-0

Asif, A.R., Sajid, M., Ahmed, W., Nawaz, A. (2024). Weathering effects on granitic rocks in North Pakistan: petrographic insights, strength classifications, and construction suitability. Environmental Earth Sciences, 83, 351. https://doi.org/10.1007/s12665-024-11655-6

Asif, A.R, Shah, S.S.A., Khan, J. (2021). The New Empirical Formulae for predicting the Unconfined Compressive Strength of limestone from Kohat Basin, Pakistan. Journal of Himalayan Earth Sciences, 54, 33-43

Bard, J.P. (1983). Metamorphism of an obducted island arc: example of the Kohistan sequence (Pakistan) in the Himalayan collided range. Earth and Planetary Science Letters, 65(1), 133-44. https://doi.org/10.1016/0012-821X(83)90195-4

Brotóns, V., Tomás, R., Ivorra, S.A., Alarcón, J.C. (2013). Temperature influence on the physical and mechanical properties of a porous rock: San Julian's calcarenite. Engineering Geology, 167, 117-27. https://doi.org/10.1016/j.enggeo.2013.10.012

Burg, J.P. (2018). Geology of the onshore Makran accretionary wedge: Synthesis and tectonic interpretation. Earth-Science Reviews, 185, 1210-31. https://doi.org/10.1016/j.earscirev.2018.09.011

Cawood, P.A., Johnson, M.R., Nemchin, A.A. (2007). Early Palaeozoic orogenesis along the Indian margin of Gondwana: Tectonic response to Gondwana assembly. Earth and Planetary Science Letters, 255(1-2), 70-84

https://doi.org/10.1016/j.epsl.2006.12.006

Chaki, S., Takarli, M., Agbodjan, W.P. (2008). Influence of thermal damage on physical properties of a granite rock: porosity, permeability and ultrasonic wave evolutions. Construction Building Materials, 22(7), 1456-61. https://doi.org/10.1016/j.conbuildmat.2007.04.002

Chen, X., Liao, Z., Peng, X. (2012). Deformability characteristics of jointed rock masses under uniaxial compression. International Journal of Mining Science Technology, 22(2), 213-21. https://doi.org/10.1016/j.ijmst.2011.08.012

Coward, M.P., Butler, R.W.H., Khan, M.A., Knipe, R.J. (1987). The tectonic history of Kohistan and its implications for Himalayan structure. Journal of Geological Society, 144(3), 377-391. https://doi.org/10.1144/gsjgs.144.3.0377

Dhuime, B., Bosch, D., Bodinier, J.L., Garrido, C.J., Bruguier, O., Hussain, S.S., Dawood, H. (2007). Multistage evolution of the Jijal ultramafic–mafic complex (Kohistan, N Pakistan). implications for building the roots of island arcs. Earth and Planetary Science Letters, 261(1-2), 179-200. https://doi.org/10.1016/j.epsl.2007.06.026

DiPietro, J.A., Ahmad, I., Hussain, A. (2008). Cenozoic kinematic history of the Kohistan fault in the Pakistan Himalaya. Geological Society of America Bulletin, 120(11-12), 1428-40. https://doi.org/10.1130/B26204.1

Ersoy, H., Kolaylı, H., Karahan, M., Karahan, H.H., Sünnetci, M.O. (2019). Effect of thermal damage on mineralogical and strength properties of basic volcanic rocks exposed to high temperatures. Bulletin of Engineering Geology and the Environment, 78(3), 1515-1525. https://doi.org/10.1007/S10064-017-1208-Z

Feng, G., Zhu, C., Wang, X., & Tang, S. (2023). Thermal effects on prediction accuracy of dense granite mechanical behaviors using modified maximum tangential stress criterion. Journal of Rock Mechanics and Geotechnical Engineering, 15(7), 1734-1748. https://doi.org/10.1016/j.jrmge.2022.12.003

Ferrero, A.M., and P. Marini. (2001). Experimental studies on the mechanical behaviour of two thermal cracked marbles. Rock Mechanics and Rock Engineering, 34:57–66. https://doi.org/10.1007/s006030170026

Gomah, M. E., Li, G., Omar, A. A., Abdel Latif, M. L., Sun, C., & Xu, J. (2024). Thermal-Induced Microstructure Deterioration of Egyptian Granodiorite and Associated Physico-Mechanical Responses. Materials, 17(6), 1305. https://doi.org/10.3390/ma17061305

Hu, X., Lacidogna, G., Xie, N., Montanari, P. M., & Gong, X. (2024). Tensile Microcracking Behavior of Granites After High Temperature Treatment by Considering the Effect of Grain Size and Mineralogical Composition. Rock Mechanics and Rock Engineering, 1-27. https://doi.org/10.1007/s00603-024-04108-w

Huang, C., Zhu, C., & Ma, Y. (2025). Investigating Mechanical Characteristics of Rocks Under Freeze–Thaw Cycles Using Grain-Based Model. Rock Mechanics and Rock Engineering, 58(1), 603-622. https://doi.org/10.1007/s00603-024-04154-4

Huang, S., Xia, K. (2015). Effect of heat-treatment on the dynamic compressive strength of Longyou sandstone. Engineering Geology, 191, 1-7. https://doi.org/10.1016/j.enggeo.2015.03.007

Jan, M.Q. (1988). Geochemistry of amphibolites from the southern part of the Kohistan arc, N. Pakistan. Mineral Magazine, 52(365), 147-159. https://doi.org/10.1180/minmag.1988.052.365.02

Jan, M.Q., Howie, R. (1981). The mineralogy and geochemistry of the metamorphosed basic and ultrabasic rocks of the Jijal complex, Kohistan, NW Pakistan. Journal of Petrology, 22(1), 85-126. https://doi.org/10.1093/petrology/22.1.85

Jiang, S., Chen, C., Zhang, S., Xu, Z., Liu, X., Tu, G., & Zhao, S. (2025). Thermo-Hydro-Mechanical coupling analysis of spiral wellbores in horizontal wells for heat extraction from hot dry rock: A case study of the Gonghe Basin, Qinghai, China. Energy, 135058. https://doi.org/10.1016/j.energy.2025.135058

Kanu, A.B., Dwivedi, P., Tam, M., Matz, L., Hill, H.H. (2008). Ion mobility–mass spectrometry. Journal of Mass Spectrometry, 43(1), 1-22. https://doi.org/10.1002/jms.1383

Khan, H., Sajid, M. (2023). Investigating the textural and physico-mechanical response of granites to heat treatment. International Journal of Rock Mechanics and Mining Sciences, 161, 105281. https://doi.org/10.1016/j.ijrmms.2022.105281

Khan, M.A., Jan, M.Q., Weaver, B.L. (1993). Evolution of the lower arc crust in Kohistan, N. Pakistan: temporal arc magmatism through early, mature and intra-arc rift stages. Geological Society Special Publications, 74(1), 123-38. https://doi.org/10.1144/GSL.SP.1993.074.01.10

Kibikas, W. M., Ghassemi, A., Choens, R. C., Bauer, S. J., Shalev, E., & Lyakhovsky, V. (2025). Thermophysical properties of the Ghareb formation relevant for nuclear waste disposal. Acta Geotechnica, 1-18. https://doi.org/10.1007/s11440-025-02535-9

King, J., Harris, N., Argles, T., Parrish, R., Zhang, H. (2011). Contribution of crustal anatexis to the tectonic evolution of Indian crust beneath southern Tibet. Bulletin, 123(1-2), 218-39. https://doi.org/10.1130/B30085.1

Le Fort, P. (1986). Metamorphism and magmatism during the Himalayan collision. Geological Society Special Publications, 19(1), 159-172.

Li, J., Bai, J., Feng, G., Han, Y., Wu, G., Ma, J., ... & Mi, J. (2024). A high temperature resistance backfilling material for underground coal gasification: Microstructure, physical and mechanical characteristics. Construction and Building Materials, 441, 137557. https://doi.org/10.1016/j.conbuildmat.2024.13755

Lion, M., Skoczylas, F., Ledésert, B. (2005). Effects of heating on the hydraulic and poroelastic properties of bourgogne limestone. International Journal of Rock Mechanics and Mining Sciences, 42(4), 508-20. https://doi.org/10.1016/j.ijrmms.2005.01.005

Long, K., Wei, Q., Peng, K., Wu, Y., Luo, S., Cheng, Y., & Li, L. (2024). Cracking process and microstructural characteristics of granite under heating–cooling alternations. Physics of Fluids, 36(3). https://doi.org/10.1063/5.0194662

Ma, G., Li, J., Zhao, Y., Zhou, X., Qiu, P., & Lu, J. (2024). Effect of heat treatment on the shear fracture and acoustic emission properties of granite with thermal storage potential: A laboratory-scale test. Theoretical and Applied Fracture Mechanics, 133, 104621. https://doi.org/10.1016/j.tafmec.2024.104621

Mao, X.B., Zhang, L.Y., Li, T.Z., Liu, H.S. (2009). Properties of failure mode and thermal damage for limestone at high temperature. Mining Science and Technology, 19(3), 290-4. https://doi.org/10.1016/S1674-5264(09)60054-5

Noble, S.R., Searle, M.P., Walker, C.B. (2001). Age and tectonic significance of Permian granites in western Zanskar,

High Himalaya. The Journal of Geology, 109(1), 127-35. https://www.jstor.org/stable/10.1086/jg.2001.109.issue-1

Ozguven, A., Ozcelik, Y. (2013). Investigation of some property changes of natural building stones exposed to fire and high heat. Construction and Building Materials, 38, 813-821. https://doi.org/10.1016/j.conbuildmat.2012.09.072

Pan, J., Ma, Y., Zhang, L., Xi, X., Zhang, Y., & Cai, M. (2024). Effect of heat treatment on microcracking behaviors and Mode-I fracture characteristics of granite: An experimental and numerical investigation. Theoretical and Applied Fracture Mechanics, 104489. https://doi.org/10.1016/j.tafmec.2024.104489

Qiao, J., Wang, G., Song, L., Liu, X., Zhou, C., Niu, Y., & Liu, B. (2024). Mechanical properties and the mechanism of microscopic thermal damage of basalt subjected to high-temperature treatment. Natural Hazards, 120(1), 41-61. https://doi.org/10.1007/s11069-023-06191-8

Reuschlé, T., Haore, S.G., Darot, M. (2006). The effect of heating on the microstructural evolution of La Peyratte granite deduced from acoustic velocity measurements. Earth and Planetary Science Letters, 243(3-4), 692-700. https://doi.org/10.1016/j.epsl.2006.01.038

Ringuette, L., Martignole, J., Windley, B.F. (1999). Magmatic crystallization, isobaric cooling, and decompression of the garnet-bearing assemblages of the Jijal sequence (Kohistan terrane, western Himalayas). Geology, 27(2), 139-42.

Rong, G., Peng, J., Yao, M., Jiang, Q., Wong, L.N. (2018). Effects of specimen size and thermal-damage on physical and mechanical behavior of a fine-grained marble. Engineering Geology, 232, 46-55. https://doi.org/10.1016/j.enggeo.2017.11.011

Sajid, M., Andersen, J., Rocholl, A., & Wiedenbeck, M. (2018). U-Pb geochronology and petrogenesis of peraluminous granitoids from northern Indian plate in NW Pakistan: Andean type orogenic signatures from the early Paleozoic along the northern Gondwana. Lithos, 318, 340-356. https://doi.org/10.1016/j.lithos.2018.08.024

Searle, M.P, Khan, M.A., Fraser, J.E., Gough, S.J., Jan, M.Q. (1999). The tectonic evolution of the Kohistan-Karakoram collision belt along the Karakoram Highway transect, north Pakistan. Tectonics, 18(6), 929-49. https://doi.org/10.1029/1999TC900042

Searle, M.P. (2011). Geological evolution of the Karakoram Ranges. Italian Journal of Geosciences, 130(2), 147-59. https://doi.org/10.3301/IJG.2011.08

Searle, M.P., Treloar, P.J. (2010). Was Late Cretaceous–Paleocene obduction of ophiolite complexes the primary cause of crustal thickening and regional metamorphism in the Pakistan Himalaya? Geological Society Special Publication, 338(1), 345-59. https://doi.org/10.1144/SP338.16

Shahbazi, M., Najafi, M., Marji, M. F., & Rafiee, R. (2024). A thermo-mechanical simulation for the stability analysis of a horizontal wellbore in underground coal gasification. Petroleum, 10(2), 243-253. https://doi.org/10.1016/j.petlm.2023.11.003

Si, X., Luo, Y., Gong, F., Huang, J., & Han, K. (2024). Temperature effect of rockburst in granite caverns: insights from reduced-scale model true-triaxial test. Geomechanics and Geophysics for Geo-Energy and Geo-Resources, 10(1), 26. https://doi.org/10.1007/s40948-024-00736-2

Sirdesai, N.N., Singh, A., Sharma, L.K., Singh, R., Singh, T.N. (2018). Determination of thermal damage in rock specimen using intelligent techniques. Engineering Geology, 239, 179-94. https://doi.org/10.1016/j.enggeo.2018.03.027

Treloar, P.J, Broughton, R.D., Williams, M.P., Coward, M.P., Windley, B.F. (1989). Deformation, metamorphism and imbrication of the Indian plate, south of the Main Mantle Thrust, north Pakistan. Journal of Metamorphic Geology, 7(1), 111-25. https://doi.org/10.1111/j.1525-1314.1989.tb00578.x

Treloar, P.J., Petterson, M.G., Jan, M.Q., Sullivan, M.A. (1996). A re-evaluation of the stratigraphy and evolution of the Kohistan arc sequence, Pakistan Himalaya: implications for magmatic and tectonic arc-building processes. Journal of the Geological Society, 153(5), 681-93. https://doi.org/10.1144/gsjgs.153.5.0681

Vázquez, P., Shushakova, V., Gómez-Heras, M. (2015). Influence of mineralogy on granite decay induced by temperature increase: Experimental observations and stress simulation. Engineering Geology, 189, 58-67. https://doi.org/10.1016/j.enggeo.2015.01.026

Wang, L., Wu, Y., Huang, Z., Lin, J., Wang, Y., & Zhang, W. (2024). Effects of temperature and confining pressure on the permeability of Beishan granite from high-level radioactive waste disposal repository. Case Studies in Thermal Engineering, 55, 104111. https://doi.org/10.1016/j.csite.2024.104111

Wang, Y., Xing, X., Cawood, P.A., Lai, S., Xia, X., Fan, W., Liu, H., Zhang, F. (2013). Petrogenesis of early Paleozoic peraluminous granite in the Sibumasu Block of SW Yunnan and diachronous accretionary orogenesis along the northern margin of Gondwana. Lithos, 182, 67-85. https://doi.org/10.1016/j.lithos.2013.09.010

Wang, Z., Chen, F., Dong, Z., Li, H., Shi, X., Xu, Z., ... & Yang, C. (2024). Study on the influence of temperature on the damage evolution of hot dry rock in the development of geothermal resources. Geoenergy Science and Engineering, 241, 213171. https://doi.org/10.1016/j.geoen.2024.213171

Wong, L. N. Y., Zhang, Y., Cui, X., & Wu, Z. (2024). Thermal effect on rock strength: strengthening-weakening transition explored by grain-based model. Acta Geotechnica, 19(6), 3321-3336. https://doi.org/10.1007/s11440-023-02049-2

Wu, L., Huang, Y., Li, J., Wang, G., Li, Y., Li, X., ... & Ji, C. (2025). Macro-and micro-mechanical response and damage mechanism of sandstone under high-temperature conditions. International Journal of Mining Science and Technology. https://doi.org/10.1016/j.ijmst.2025.01.004

Yavuz, H., Demirdag, S., Caran, S. (2010). Thermal effect on the physical properties of carbonate rocks. International Journal of Rock Mechanics and Mining Sciences, 47(1), 94-103. https://doi.org/10.1016/j.ijrmms.2009.09.014

Yin, W., Feng, Z., & Zhao, Y. (2024). Investigation on the characteristics of hydraulic fracturing in fractured-subsequently-filled hot dry rock geothermal formation. Renew-

able Energy, 223, 120061. https://doi.org/10.1016/j.renene.2024.120061

Zeitler, P.K. (1985). Cooling history of the NW Himalaya, Pakistan. Tectonics, 1, 127-51. https://doi.org/10.1029/TC004i001p00127

Zhang, L., Mao, X., Lu, A. (2009). Experimental study on the mechanical properties of rocks at high temperature. Science in China Series E: Technological Sciences, 52, 641–646. https://doi.org/10.1007/s11431-009-0063-y

Zhang, L., Yang, D., Zhao, K., Zhao, Y., Jin, J., Wang, X., ... & Li, C. (2024). Investigation of high-temperature effects on the strengthening and degradation of mechanical property in sandstone. Applied Energy, 357, 122532. https://doi.org/10.1016/j.apenergy.2023.122532

SAŽETAK

Utjecaj različitih temperatura na oštećenje stijena: razvoj pukotina i određivanje fizičkih i mehaničkih svojstava

Razumijevanje učinaka visokih temperatura na fizička i mehanička svojstva stijena bitno je za procjenu njihova ponašanja u ekstremnim uvjetima i optimizaciju inženjerskih zahvata. Temperatura znatno utječe na svojstva, bilo da ih poboljšava ili degradira, a ovisno o mineraloškome sastavu stijena. Ovim radom prikazano je detaljno istraživanje utjecaja visokih temperatura na fizička i mehanička svojstva različitih vrsta stijena, uključujući vapnenac, pješčenjak, gnajs, riolit, kvarcit, dolerit, gabronorit, amfibolit i granulit. Uzorci stijena bili su izloženi temperaturama od 150 °C do 1000 °C. Potom su provedena destruktivna (jednoosna tlačna čvrstoća, indeks opterećenja u točki) i nedestruktivna ispitivanja (specifična težina, brzina prolaza ultrazvučnih valova, poroznost i upijanje vode) kako bi se procijenilo ponašanje stijena u ovisnosti o različitim temperaturama. Za svaku vrstu stijene pri ispitivanim temperaturama izračunana je gustoća induciranih pukotina uslijed temperaturnoga šoka. Rezultati su pokazali smanjenje jednoosne tlačne čvrstoće, specifične težine, ultrazvučne brzine i čvrstoće opterećenja u točki s porastom temperature. Suprotno tome, s povišenjem temperature povećala se gustoća pukotina, poroznost i količina upijene vode. Primjetna i nagla promjena svih svojstava uočena je kada temperatura prijeđe 300 °C. Ti rezultati naglašavaju propadanje stijena i promjene u njihovim fizičkim i mehaničkim svojstvima uzrokovanim izlaganju toplini, što ima ključnu važnost u industriji poput rudarstva i građevinarstva. Kombinirajući dobivene rezultate fizičkih i mehaničkih svojstava na različitim temperaturama, izvedene su jednadžbe za svaku vrstu stijene. Jednadžbe se mogu koristiti prilikom procjene odgovarajućih svojstava na željenim temperaturama. Ovaj je rad važan za razumijevanje kako izloženost toplini utječe na cjelovitost stijena, pružajući ključan uvid za industrije kao što su rudarstvo, građevinarstvo i geotermalna energija. Omogućuje bolje predviđanje i upravljanje ponašanjem stijene u uvjetima visokih temperatura povećavajući sigurnost i izvedbu u inženjerskim primjenama.

Ključne riječi:
termička obrada, toplinski utjecaj, fizička i mehanička svojstva, stijene, termička degradacija, jednadžbe

Author's contribution

Abid Nawaz (PhD Scholar) contributed to the conceptualization, methodology, field investigation, data curation, and writing the original draft. **Muhammad Sajid** (PhD, Assistant Professor) and **Waqas Ahmed** (PhD, Associate Professor) contributed to reviewing and editing, supervision, and funding acquisition. **Abdul Rahim Asif** (PhD, Lecturer) contributed to field investigation, laboratory work, and data support.
All authors have read and agreed to the published version of the manuscript.